Available online at www.sciencedirect.com

Materials Chemistry and Physics 90 (2005) 62–68

MATERIALS CHEMISTRY AND PHYSICS

www.elsevier.com/locate/matchemphys

Luminescence characteristics of europium-ion doped $BaMgAl_{10}O_{17}$ phosphors prepared via a sol–gel route employing polymerizing agents

Chung-Hsin Lu[a,*], Wei-Tse Hsu[a], Chien-Hao Huang[a], S.V. Godbole[a], Bing-Ming Cheng[b]

[a] *Department of Chemical Engineering, National Taiwan University, No. 1, Sec. 4, Roosevelt Road, Taipei, Taiwan*
[b] *National Synchrotron Radiation Research Center, Hsinchu, Taiwan*

Received 30 May 2004; received in revised form 29 September 2004; accepted 30 September 2004

Abstract

Europium-ion doped $BaMgAl_{10}O_{17}$ phosphors were prepared via both a sol–gel route and the conventional solid-state route. The effects of various preparation conditions on the optical properties of $BaMgAl_{10}O_{17}$ based phosphors were investigated. The position of charge transfer band and emission characteristics of europium ions in $Ba_{0.9}Eu_{0.1}MgAl_{10}O_{17}$ are observed to be different between those prepared by the sol–gel route and those derived from the solid-state route. The sites occupied by europium ions in $BaMgAl_{10}O_{17}$ are found to depend upon the method of synthesis. The ratios of the intensity of 610 nm emission ($^5D_0 \rightarrow {}^7F_2$) to that of 590 nm emission ($^5D_0 \rightarrow {}^7F_1$) suggest that Eu^{3+} ions are located in a more asymmetric environment for the sol–gel-derived phosphors as compared to that in phosphors prepared via the solid-state route. VUV-excited emission characteristics indicate that the prepared phosphors generate intense emission at 458 nm under excitation at 147 nm. In addition, the luminescence intensity of the sol–gel-derived phosphors is greater than that of the solid-state-route-derived phosphors. The sol–gel method employing polymerizing agents is demonstrated to be suitable for the synthesis of phosphors used in plasma display panels.

Keywords: Sol–gel; Phosphor; Luminescence; Barium magnesium aluminate

1. Introduction

$BaMgAl_{10}O_{17}$ is one of the important phosphors utilized in luminescent devices [1,2]. Recently, increasing attention is being paid to $BaMgAl_{10}O_{17}$: Eu^{2+} phosphors owing to their application in plasma display panels (PDP) as the blue-light components. It is reported that UV light and temperature-induced degradation is more predominant for $BaMgAl_{10}O_{17}$: Eu^{2+} phosphors as compared to the red and green emitting phosphors in the tri-color blend [3–5]. The results of Mossabauer spectroscopic studies and theoretical calculations of energy levels based on molecular orbital approach indicate that Eu^{2+} ions occupy three sites in $BaMgAl_{10}O_{17}$ [6,7]. Thermal degradation in $BaMgAl_{10}O_{17}$ is also noted to vary among the three sites [7]. The different sites for Eu^{2+} ions are also supported by the luminescence investigations of Sm^{2+} doped $BaMgAl_{10}O_{17}$ [8]. Due to the different heating conditions, Eu^{3+} are also possibly existent in $BaMgAl_{10}O_{17}$. However, the influence of heating conditions on the luminescence properties of $BaMgAl_{10}O_{17}$ has not been investigated in detail. The investigation of the spectra of Eu^{3+} ions can provide structural information of the host.

For investigating the luminescence properties of $BaMgAl_{10}O_{17}$ phosphors, two synthesis processes viz. the sol–gel route incorporating polymerizing agents and the solid-state reaction route are adopted in this study. The synthesis and characterization of $Ba_{0.9}Eu_{0.1}MgAl_{10}O_{17}$ phosphors prepared by both processes are reported. The influence of the heating conditions and preparation methods on the phase formation is explored. The effects of heating atmosphere on the luminescence properties of the phosphors are investigated. The luminescence properties of the phosphors prepared via the above processes are compared. To further examine the feasibility of the prepared phosphors for the applications to PDP devices, VUV-excited

---

[*] Corresponding author. Tel.: +886 223651428; fax: +886 223651428.
E-mail address: chlu@ccms.ntu.edu.tw (C.-H. Lu).

0254-0584/$ – see front matter © 2004 Elsevier B.V. All rights reserved.
doi:10.1016/j.matchemphys.2004.09.031

luminescence is investigated employing high-intensity synchrotron radiation facilities.

2. Experimental

Analytical grade barium oxide (BaO), magnesium oxide (MgO), aluminum oxide (Al_2O_3), and europium oxide (Eu_2O_3) were used as the starting materials in the solid-state reactions. The above four oxides were mixed according to the chemical formula $Ba_{0.9}Eu_{0.1}MgAl_{10}O_{17}$. These oxides were ball-milled with ethyl alcohol using zirconia (ZrO_2) balls for 48 h. The slurry was subsequently dried in a vacuum dryer. The dried precursors were fired at 1500 °C for 4 and 12 h in air. $Ba_{0.9}Eu_{0.1}MgAl_{10}O_{17}$ powders obtained after 4 and 12 h calcination in air via the conventional solid-state reaction route are henceforth called as C-A-4 and C-A-12, respectively. The phase purity of the obtained powders was confirmed via XRD analysis. The reduction of Eu^{3+} ions to Eu^{2+} ions was achieved via heating the precursors in the reducing atmosphere of N_2 (95 vol.%) and H_2 (5 vol.%) at 1400 °C for 4 h. The powders derived from the precursors C-A-12 after reduction is henceforth called C-R-12. The preparation conditions and the nomenclature used for identification for $Ba_{0.9}Eu_{0.1}MgAl_{10}O_{17}$ phosphors obtained via the conventional solid-state route and the sol–gel route involving various stages of heating are listed in Table 1.

The synthesis procedures in the sol–gel process employing citric acid and ethylene glycol are summarized in the flowchart illustrated in Fig. 1. Analytical grade nitrates dissolved in deionized water were used as the starting materials for Ba^{2+} (0.09 M), Al^{3+} (1.0 M), and Mg^{2+} (0.1 M) ions. Europium nitrate solution was obtained by dissolving analytical grade Eu_2O_3 in dilute nitric acid. Citric acid was used as chelating agent; while, ethylene glycol was used as polymerizing agent. Homogeneous colorless solution was observed after continuous stirring for 1.5 h. After adding ethylene glycol into the clear solution, the mixture was continuously stirred and heated at 130 °C. At this stage, excess water was evaporated from the mixture. When the mixture was heated at 300 °C for 1.5 h, white gels were obtained. The powders obtained via grinding the gels were further calcined at select temperatures for 4 h in air. The sol–gel-derived precursors after heating in air at 800, 1000, 1200, and 1400 °C are henceforth termed as S-A-8, S-A-10, S-A-12, and S-A-14, respectively. The formation of Eu^{2+} ions in the phosphors was achieved by heating the sol–gel-derived precursors in the reducing atmosphere as mentioned in earlier section. $Ba_{0.9}Eu_{0.1}MgAl_{10}O_{17}$ phosphors obtained from reducing the precursors S-A-8, S-A-10, S-A-12, and S-A-14 are henceforth named as S-R-8, S-R-10, S-R-12, and S-R-14, respectively. To investigate the effect of thermal degradation, the sol–gel-derived (S-R-14) and conventionally prepared (C-R-12) $Ba_{0.9}Eu_{0.1}MgAl_{10}O_{17}$ phosphors were heated further in air at 500 °C for 1 h. $Ba_{0.9}Eu_{0.1}MgAl_{10}O_{17}$ phosphors obtained from the precursors S-R-14 and C-R-12 after the third stage heating in air are henceforth named as S-T-14 and C-T-12, respectively.

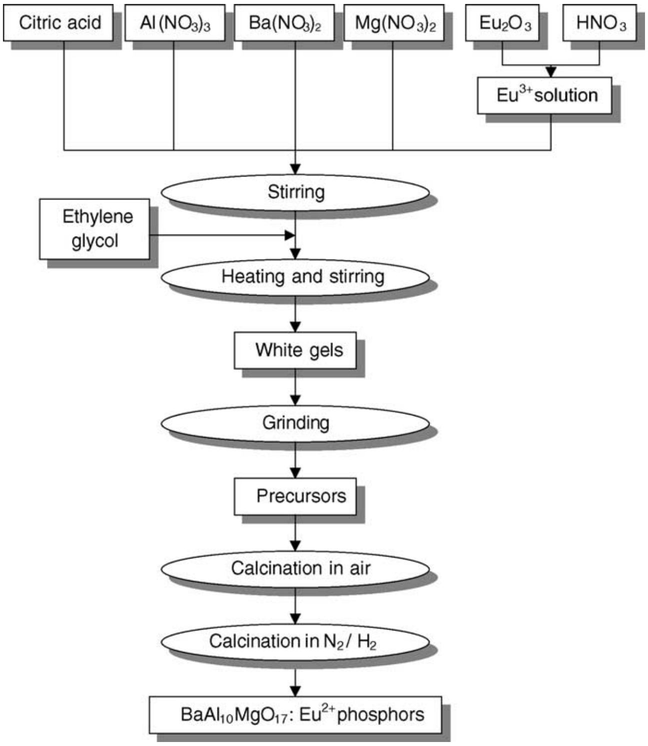

Fig. 1. Flowchart for the synthesis of sol–gel-derived $Ba_{0.9}Eu_{0.1}MgAl_{10}O_{17}$ phosphors employing citric acid and ethylene glycol.

X-ray diffraction patterns for the prepared powders were detected via a X-ray diffractometer (MAC M03 XHF) using Cu Kα. A field emission scanning electron microscope (Hitachi S-800) was used to observe the microstructures of the prepared powders. UV-induced luminescence studies were conducted using a fluorescence spectrometer (Hitachi F-4500). VUV-induced luminescence studies were performed using synchrotron radiation facility (National Synchrotron Radiation Research Center, Hsin-Chiu, Taiwan). The synchrotron radiation facility enabled recording of VUV excitation spectra in 120–200 nm and VUV-excited emission spectra in 300–800 nm.

3. Results and discussion

3.1. Sample characterization and morphology of the prepared phosphors

Fig. 2 illustrates the XRD patterns for the representative powders obtained during synthesis. In particular, Fig. 2(a)–(c) illustrate the XRD patterns for $Ba_{0.9}Eu_{0.1}MgAl_{10}O_{17}$ phosphors prepared via the solid-state reaction, the sol–gel-derived powders after calcination in air, and the sol–gel-derived powders obtained after the reducing treatment, respectively. Fig. 2(a) demonstrates that powders (C-A-12)

Table 1
Preparation conditions and sample nomenclature for identification in three stage preparation via different routes for $Ba_{0.9}Eu_{0.1}MgAl_{10}O_{17}$ phosphors

Preparation conditions for samples	First-stage heating (in air at selected temperatures)	Second-stage heating (in reducing atmosphere at 1400 °C)	Third-stage heating (in air at 500 °C)
Solid-state route	C-A-4 (1500 °C for 4 h)		
	C-A-12 (1500 °C for12 h)	C-R-12 (via heating C-A-12)	C-T-12 (via heating C-R-12)
Sol–gel route	S-A-8 (800 °C for 4 h)	S-R-8 (via heating S-A-8)	
	S-A-10 (1000 °C for 4 h)	S-R-10 (via heating S-A-10)	
	S-A-12 (1200 °C for 4 h)	S-R-12 (via heating S-A-12)	
	S-A-14 (1400 °C for 4 h)	S-R-14 (via heating S-A-14)	S-T-14 (via heating S-R-14)

obtained via the solid-state route after heating at 1500 °C for 12 h (curve ii) are corresponding to pure $BaMgAl_{10}O_{17}$ (ICDD No. 26-0163) [9]; while, an unknown phase is present in the powders (C-A-4) derived after heating at 1500 °C for 4 h (curve i). For the synthesis of pure-phase BAM phosphors via solid-state reactions, prolonged heating is required.

Fig. 2(b) depicts the XRD patterns for the sol–gel-derived $Ba_{0.9}Eu_{0.1}MgAl_{10}O_{17}$ phosphors obtained after heating in air for 4 h at selected temperatures. The XRD patterns for $Ba_{0.9}Eu_{0.1}MgAl_{10}O_{17}$ powders obtained via heating at 800 °C (S-A-8), 1000 °C (S-A-10), 1200 °C (S-A-12), and 1400 °C (S-A-14) are illustrated in curves iii, iv, v, and vi, respectively. Curve (iii) indicates the formation of $BaAl_2O_4$ (BAL) during the first stage of heating in air at 800 °C [10]. Powders obtained via heating at 1000 °C reveal an increase in the crystallinity of $BaAl_2O_4$ phase and absence of secondary phases. In the sol–gel-derived phosphors, $BaMgAl_{10}O_{17}$ is obtained as the product (curve v) along with the impurity phase $BaAl_2O_4$. $Ba_{0.9}Eu_{0.1}MgAl_{10}O_{17}$ exhibiting the diffraction patterns corresponding to $BaMgAl_{10}O_{17}$ is observed to coexist with a trace of Eu_2O_3 [11] phase after calcination at 1400 °C in air (curve vi).

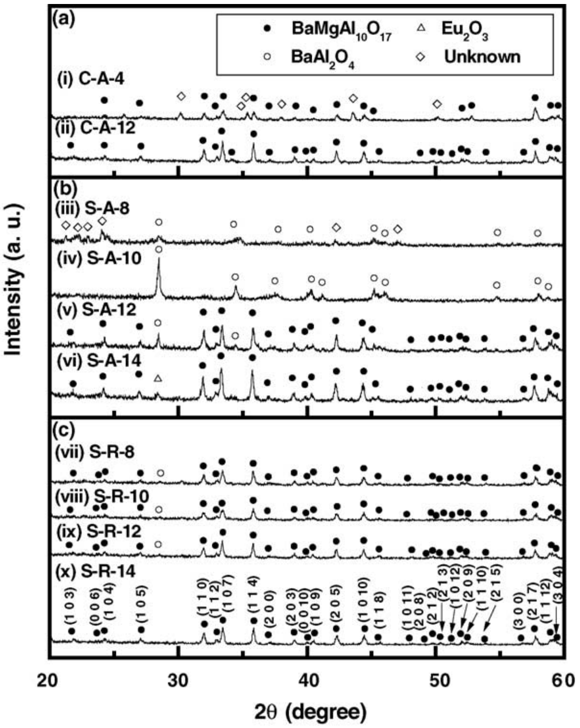

Fig. 2. XRD patterns for $Ba_{0.9}Eu_{0.1}MgAl_{10}O_{17}$ phosphors obtained via (a) the solid-state route by heating at 1500 °C in air (i) for 4 h and (ii) 12 h; (b) the sol–gel route obtained after calcination in air at (iii) 800 °C, (iv) 1000 °C, (v) 1200 °C, and (vi) 1400 °C; and (c) heating in the reducing atmosphere for the sol–gel-derived precursors calcined in air at (vii) 800 °C, (viii) 1000 °C, (ix) 1200 °C, and (x) 1400 °C.

Fig. 2(c) illustrates the XRD patterns for the sol–gel-derived powders obtained after heating the precursors shown in Fig. 2(b) at 1400 °C for 4 h in the reducing atmosphere. Owing to the heat treatment at 1400 °C, all powders contain $BaMgAl_{10}O_{17}$ phase (curves vii–x); however, S-R-14 (curve x) is the only sample that resulted in single-phase $BaMgAl_{10}O_{17}$ powders without traces of $BaAl_2O_4$ and Eu_2O_3. These observations suggest that raising the calcination temperature in the first stage of heating can facilitate the synthesis of $Ba_{0.9}Eu_{0.1}MgAl_{10}O_{17}$ phosphors for obtaining pure-phase compound.

Fig. 3 illustrates the microstructures observed for the sol–gel-derived $Ba_{0.9}Eu_{0.1}MgAl_{10}O_{17}$ powders prepared via (a) calcining precursors at 1400 °C in air (S-A-14) and (b) powders (S-R-14) obtained via heating in the reducing atmosphere of the precursors (S-A-14). The samples prepared via the sol–gel route exhibit irregular shapes. In general, particles of 4–6 μm in size are obtained via the sol–gel route incorporating polymerizing agents. In comparison with the reported particle size for powders synthesized via the sol–gel route without polymerizing agents, the particle sizes observed in the present studies are relatively smaller [12].

3.2. UV-induced luminescence characteristics of Eu^{3+} and Eu^{2+} ions in $BaMgAl_{10}O_{17}$

Eu^{2+} doped $BaMgAl_{10}O_{17}$ phosphors are known to emit in blue region on excitation with UV light [6,12]. For the sol–gel-derived precursors heated in air, the emission in blue region is not observed. This observation indicates that for the samples prepared in air, europium ions do not incorporate as Eu^{2+} ions in the host. Fig. 4 shows the excitation and emission spectra recorded for $Ba_{0.9}Eu_{0.1}MgAl_{10}O_{17}$ phosphors prepared in air via the solid-state reaction route and the sol–gel route. Based on the emission characteristics shown in Fig. 4, it is revealed that europium ions are present as Eu^{3+}

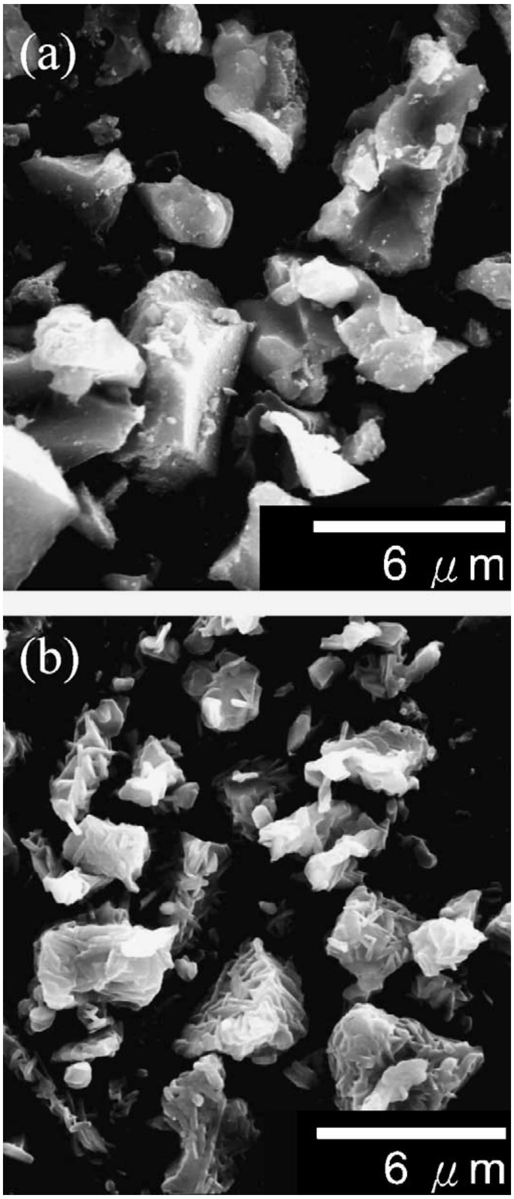

Fig. 3. SEM micrographs for $Ba_{0.9}Eu_{0.1}MgAl_{10}O_{17}$ obtained via (a) the sol–gel route after calcination in air at 1400 °C (S-A-14) and (b) heating in the reducing atmosphere for the sol–gel-derived precursors calcined in air at 1400 °C (S-R-14).

ions in the prepared phosphors. Curve (a) illustrates the luminescence characteristics for sample C-A-12 prepared via the solid-state reaction route. The excitation spectra for the sample were recorded by monitoring emission at 590 nm; while, the emission spectra were recorded by exciting the sample at 258 nm. For the sample prepared in air, emission peaks are observed at 578, 589, 605, and 632 nm. The excitation spectra reveal broad excitation with a strong peak at 258 nm and a weak excitation peak at 395 nm (seen in the inset). From the nature and intensities of these excitation peaks, the strong and broad excitation at 258 nm can be identified as the charge transfer band; while, the weak excitation peak at 395 nm is due to intra-configurational $4f^n$ transition [13,14].

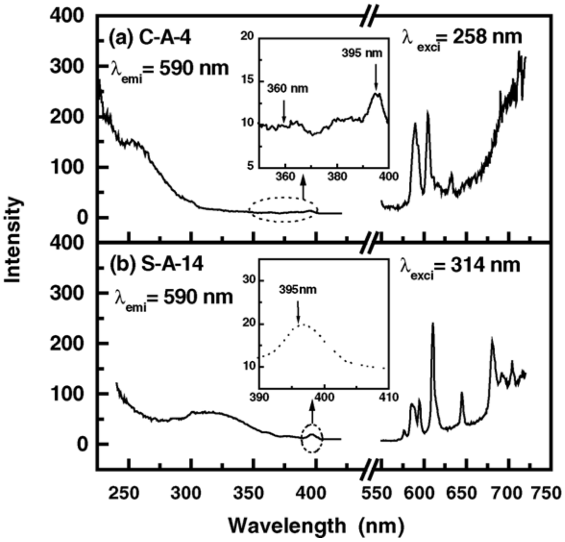

Fig. 4. Excitation ($\lambda_{emission} = 590$ nm) and emission ($\lambda_{excitation} = 258/314$ nm) spectra for Eu^{3+} ions in $Ba_{0.9}Eu_{0.1}MgAl_{10}O_{17}$ prepared in air via (a) the solid-state reactions route (C-A-12) and (b) the sol–gel route after calcinations at 1400 °C (S-A-14).

Curve (b) in Fig. 4 illustrates the excitation ($\lambda_{emission} = 590$ nm) and emission ($\lambda_{excitation} = 314$ nm) spectra recorded for the sol–gel-derived $Ba_{0.9}Eu_{0.1}MgAl_{10}O_{17}$ phosphors obtained via calcination at 1400 °C (S-A-14). The inset in curve (b) illustrates the excitation spectra for powders S-A-14 in the 360–420 nm region. The excitation spectra reveal a charge transfer band at 314 nm and a weak excitation peak at 395 nm due to f–f transitions. The excitation spectra of S-A-14 samples reveal that position of the charge transfer band shifts to 314 nm. A number of emission peaks with increased intensities are observed for the sol–gel-derived phosphors in comparison with those obtained via the solid-state route. The prominent emission peaks are found at 585, 588, 594, 610, 645, and 681 nm. The luminescence characteristics, including the position of charge transfer band and the emission characteristics such as the number of emission peaks and their relative intensities, reveal structural information regarding the sites occupied by Eu^{3+} ions in the host matrix.

The position of charge transfer band is known to be strongly dependent on the environment of Eu^{3+} ions in the host [15–17]. In particular, the distance between europium ions and oxygen ions, and the co-ordination numbers in different matrices both influence the positions of charge transfer bands. The differences in charge transfer bands between the sol–gel-derived and conventionally prepared $Ba_{0.9}Eu_{0.1}MgAl_{10}O_{17}$ phosphors reveal that Eu^{3+} ions are located at sites with different anionic environments in the host.

The emission peaks corresponding to $^5D_0 \rightarrow {}^7F_J$ transitions (where $J = 0, 1, 2, 3$, and 4) for Eu^{3+} ions are observed in $Ba_{0.9}Eu_{0.1}MgAl_{10}O_{17}$ phosphors—S-A-14. The emission spectra of the sol–gel-derived samples shown in curve (b) are different from those observed for the conventionally prepared sample illustrated in curve (a). The emission at around 590 and 610 nm can be identified to be due to $^5D_0 \rightarrow {}^7F_1$ and $^5D_0 \rightarrow {}^7F_2$ transitions, respectively. The intensity ratio (R) of the intensity of $^5D_0 \rightarrow {}^7F_2$ transition to that of $^5D_0 \rightarrow {}^7F_1$ transition is known to provide structural information such as asymmetry of the average coordination polyhedron of Eu^{3+} ions [18,19]. As calculated from the data illustrated in Fig. 4, the ratio R is 0.97 for $Ba_{0.9}Eu_{0.1}MgAl_{10}O_{17}$ phosphors prepared via the solid-state reaction route and the value of R increases to 5.25 for the sol–gel-derived phosphors calcined at 1400 °C. The significantly large value of R for the sol–gel-derived samples suggests that Eu^{3+} ions are incorporated in phosphors having asymmetric distorted environment during synthesis via the sol–gel route.

The changes observed in the luminescence characteristics of Eu^{3+} ions in the samples prepared via the solid-state route and the sol–gel route reveal that methods of preparation influence the incorporation of Eu^{3+} ions in $BaMgAl_{10}O_{17}$ by changing the sites at which Eu^{3+} ions are incorporated in the matrix. On the other hand, after C-A-12 and S-A-14 phosphors are subject to reducing treatment, the luminescence characteristics of Eu^{3+} ions are not detectable. The absence of Eu^{3+} ions in the phosphors subjected to the reducing treatment in contrast to their presence in the phosphors prepared in air suggests complete conversion to Eu^{2+} ions during heating in reducing atmosphere.

Fig. 5 illustrates the excitation ($\lambda_{emission} = 458$ nm) and emission ($\lambda_{excitation} = 330$ nm) spectra for the sol–gel-derived $Ba_{0.9}Eu_{0.1}MgAl_{10}O_{17}$ phosphors obtained via reduction by heating at 1400 °C in the reducing atmosphere (S-R-8 (curve a), S-R-10 (curve b), S-R-12 (curve c), and S-R-14 (curve d)). A strong blue emission with a peak at 458 nm is observed for these samples. The excitation spectra reveal a main peak at 330 nm. Similar excitation and emission spectra are reported for Eu^{2+} doped $BaMgAl_{10}O_{17}$ phosphors [6,12,20]. The curves (a–d) indicate that the emission intensities increase with the calcination temperatures of the precursors. The results of XRD investigations presented in Fig. 2(c) reveal that pure-phase $Ba_{0.9}Eu_{0.1}MgAl_{10}O_{17}$ phosphors are formed only for S-R-14 sample obtained via calcination of the precursor at 1400 °C. On the other hand, for samples S-R-8, S-R-10, and S-R-12, for which the precursors are calcined at temperatures lower than 1400 °C, the impurity phases are detected. The presence of impurity phases in these samples is considered to be responsible for the reduction in emission intensity. It is necessary to provide a reducing atmosphere during synthesis to produce divalent europium ions in $BaMgAl_{10}O_{17}$ phosphors.

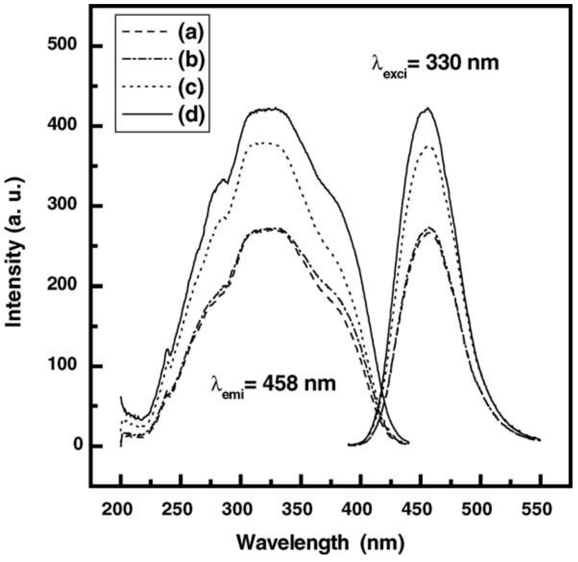

Fig. 5. Excitation ($\lambda_{emission} = 458$ nm) and emission ($\lambda_{excitation} = 330$ nm) spectra for Eu^{2+} ions in sol–gel-derived $Ba_{0.9}Eu_{0.1}MgAl_{10}O_{17}$ phosphors obtained via reduction of the precursors calcined at (a) 800 °C (S-R-8), (b) 1000 °C (S-R-10), (c) 1200 °C (S-R-12), and (d) 1400 °C (S-R-14).

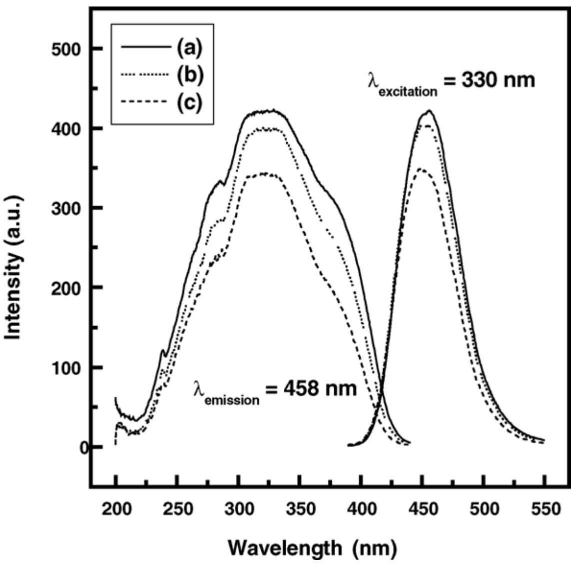

Fig. 6. Excitation ($\lambda_{emission} = 458$ nm) and emission ($\lambda_{excitation} = 330$ nm) spectra of sol–gel-derived phosphors prepared in reducing atmosphere from the precursors calcined at 1400 °C. (a) $Ba_{0.95}Eu_{0.05}MgAl_{10}O_{17}$, (b) $Ba_{0.9}Eu_{0.1}MgAl_{10}O_{17}$, and (c) $Ba_{0.85}Eu_{0.15}MgAl_{10}O_{17}$.

To understand the effect of europium content on sol–gel-derived phosphors, luminescence studies are carried out for $BaMgAl_{10}O_{17}$ with different concentrations of europium ions. Fig. 6 illustrates the excitation ($\lambda_{emission} = 458$ nm) and emission ($\lambda_{excitation} = 330$ nm) spectra recorded for $Ba_{1-x}Eu_xMgAl_{10}O_{17}$ containing different amount of x where $x = 0.05$, 0.1, and 0.15. The sol–gel-derived samples are obtained via heating the precursors in air via two-stage heating at 1400 °C in reducing atmosphere. Similar excitation and emission spectra are observed in the above three phosphors. UV-induced luminescence increases with elevated concentration of Eu^{2+} ions up to 15 at.% in $BaMgAl_{10}O_{17}$ phosphors.

Fig. 7 illustrates the excitation ($\lambda_{emission} = 458$ nm) and emission ($\lambda_{excitation} = 330$ nm) spectra recorded for $Ba_{0.9}Eu_{0.1}MgAl_{10}O_{17}$ phosphors obtained via the sol–gel route and conventional route after two-stage and three-stage

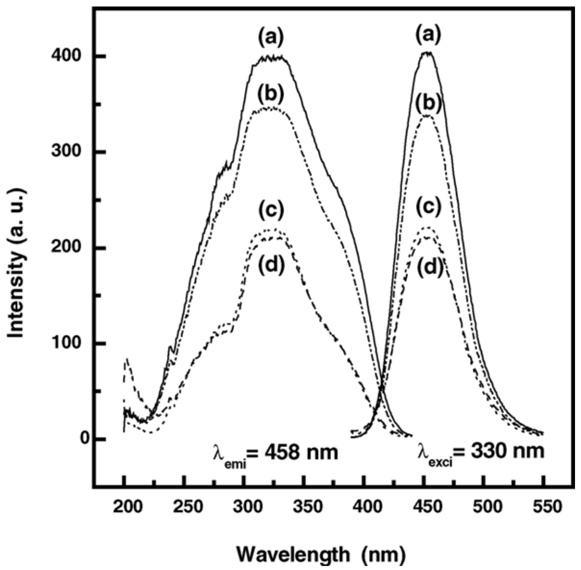

Fig. 7. Excitation ($\lambda_{\text{emission}} = 458$ nm) and emission ($\lambda_{\text{excitation}} = 330$ nm) spectra of $Ba_{0.9}Eu_{0.1}MgAl_{10}O_{17}$ phosphors prepared in the reducing atmosphere via (a) sol–gel route (S-R-14), (b) sol–gel route after third stage heating in air at 500 °C for 1 h (S-T -14), (c) solid-state route (C-R-12), and (d) solid-state route after third stage heating in air at 500 °C for 1 h (C-T-12).

heating. The luminescence characteristics of Eu^{2+} ions in $BaMgAl_{10}O_{17}$ phosphors are elucidated based on the spectra. The sol–gel-derived $Ba_{0.9}Eu_{0.1}MgAl_{10}O_{17}$ (S-R-14) phosphors (curve a) exhibits maximum intensity amongst samples shown in Fig. 7. Phosphor S-T-14 generated from all the precursor S-R-14 by heating at 500 °C for 1 h in air reveals a reduced luminescence (curve b) in comparison with that of sample S-R-14. The thermal degradation of Eu^{2+} doped $BaMgAl_{10}O_{17}$ phosphors has been reported [3–5]. The sol–gel-derived phosphors prepared with polymerizing agents are not exceptional. Curves c and d illustrate the spectra for $Ba_{0.9}Eu_{0.1}MgAl_{10}O_{17}$ phosphors prepared via the solid-state reactions after two-stage heating (C-R-12) and three-stage heating (C-T-12), respectively. For the samples prepared via the sol–gel route, emission intensities are greater than those of the sample prepared via the solid-state reaction route. Similar observation of increased luminescence for the phosphors synthesized via sol–gel route in comparison with those prepared by solid-state route has been reported by Zhang et al. [12]. The emission intensity of phosphors prepared by the conventional method also reduces due to heating in air at third stage. It is noted that sol–gel-derived $Ba_{0.9}Eu_{0.1}MgAl_{10}O_{17}$ phosphors exhibit more intense luminescence even after thermal degradation (S-T-14 (curve b)) as compared with that of phosphors prepared via the solid-state reaction (C-R-12 (curve c)). The luminescence characteristics demonstrated in Fig. 4 for the sol–gel-derived powders clearly reveal that Eu^{3+} ions are incorporated in $BaMgAl_{10}O_{17}$ phosphors at the sites having pronounced deviation from symmetry in comparison with the phosphors prepared by the solid-state route. The incorporation of Eu^{2+} ions at different sites in the precursor powders prepared by the sol–gel route facilitates an increase in the luminescence from Eu^{2+} ions.

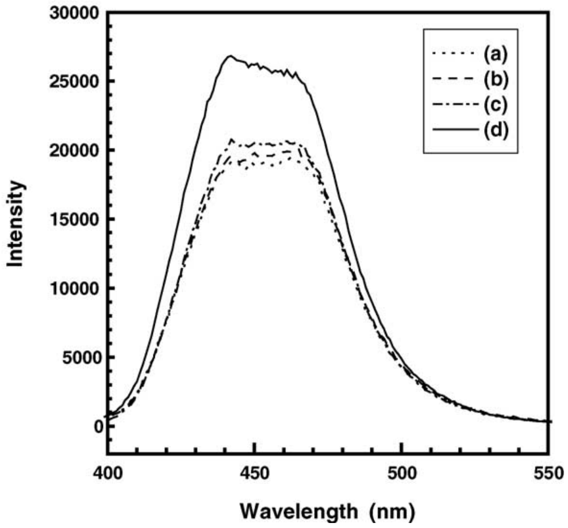

Fig. 8. Emission ($\lambda_{\text{excitation}} = 147$ nm) spectra for sol–gel-derived $Ba_{0.9}Eu_{0.1}MgAl_{10}O_{17}$ phosphors derived from reduction of the precursors calcined at (a) 800 °C (S-R-8), (b) 1000 °C (S-R-10), (c) 1200 °C (S-R-12), and (d) 1400 °C (S-R-14).

3.3. *VUV-induced luminescence characteristics of sol–gel-derived $Ba_{0.9}Eu_{0.1}MgAl_{10}O_{17}$ phosphors*

For sol–gel-derived $Ba_{0.9}Eu_{0.1}MgAl_{10}O_{17}$ phosphors, VUV-excited luminescence was investigated employing high intensity synchrotron radiation facilities. The Xe gas based discharge lamps are widely used in PDP devices as an excitation source and emit intensely at 147 nm. In order to understand the feasibility of applications in PDP devices, the emission spectra of those phosphors upon 147 nm excitation were recorded. Fig. 8 illustrates the emission ($\lambda_{\text{excitation}} = 147$ nm) spectra recorded for sol–gel-derived $Ba_{0.9}Eu_{0.1}MgAl_{10}O_{17}$ phosphors (S-R-8, S-R-10, S-R-12, and S-R-14). A broad and intense emission is observed at 458 nm for all phosphors. Similar to UV-induced luminescence shown in Fig. 5, VUV-excited emission intensity also increases with a rise in calcination temperature (curves a–d). The emission characteristics of Eu^{3+} ions are not observed upon VUV excitation for the samples obtained after the reducing treatment.

Fig. 9 illustrates the excitation ($\lambda_{\text{emission}} = 458$ nm) and emission ($\lambda_{\text{excitation}} = 147$ nm) spectra for sol–gel-derived $BaMgAl_{10}O_{17}$ phosphors with different concentrations of europium ions after calcination in the reducing atmosphere at 1400 °C. An intense VUV-excited emission in the blue region with emission peak at 458 nm is observed in all samples. The emission intensity increases with elevated concentration of europium ions up to 15 at.% in the phosphors (curve a–c). The excitation spectra reveal a strong excitation peak at 164 nm and a weak peak at 230 nm. The band-to-band excitation of

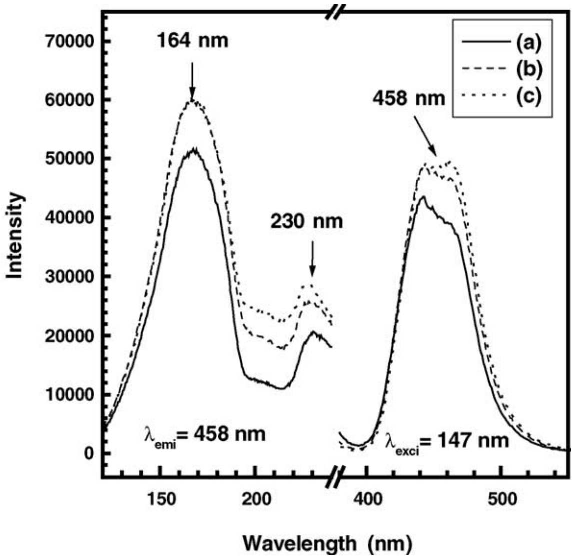

Fig. 9. Excitation ($\lambda_{\mathrm{emission}} = 458$ nm) and emission ($\lambda_{\mathrm{excitation}} = 147$ nm) spectra of sol–gel-derived phosphors prepared in reducing atmosphere from the precursors calcined at 1400 °C. (a) $Ba_{0.95}Eu_{0.05}MgAl_{10}O_{17}$, (b) $Ba_{0.9}Eu_{0.1}MgAl_{10}O_{17}$, and (c) $Ba_{0.85}Eu_{0.15}MgAl_{10}O_{17}$.

the host material results in excitation at 164 nm; while, the weak peak around 230 nm is due to $4f^7 \rightarrow 4f^6 5d^1$ transition associated with Eu^{2+} ions [20,21]. Based on the above results, it is evident that the heating conditions and the method of preparation are critical to obtain $Ba_{1-x}Eu_xMgAl_{10}O_{17}$ phosphors with intense luminescence intensity under VUV excitation for probable applications in PDP devices.

4. Conclusions

$BaMgAl_{10}O_{17}$ phosphors doped with europium ions are prepared via the sol–gel route using citric acid as a chelating agent and ethylene glycol as a polymerizing agent. The sol–gel route leads to the synthesis of pure-phase $BaMgAl_{10}O_{17}$ phosphors on calcination at 1400 °C for 4 h. The variations in the anionic environment of Eu^{3+} ions occupying different sites are reflected in the positions of charge transfer band, as well as the intensity ratios of 610 nm ($^5D_0 \rightarrow {}^7F_2$) emission to 590 nm ($^5D_0 \rightarrow {}^7F_1$) emission for the sol–gel-derived and conventionally prepared $Ba_{0.9}Eu_{0.1}MgAl_{10}O_{17}$. The europium ions of the sol–gel-derived phosphors are in a more asymmetric environment in comparison with those phosphors prepared via the solid-state route. The brightness of the sol–gel-derived phosphors is higher than that of the phosphors obtained via the solid-state route. The emission intensities of the sol–gel-derived phosphors after thermal degradation are also greater than those of the phosphors obtained via the solid-state route. The phosphors prepared via the sol–gel method employing additional polymerizing agent are found to be suitable for PDP applications.

Acknowledgements

The authors would like to thank National Science Council, Taiwan, Republic of China, for partial financial support of this study under Contract No. NSC 92-2214-E002-036. We would also like to thank Hong-Kai Chen and Hsiao-Chi Lu in National Synchrotron Radiation Research Center for their assistance in the measurement of VUV spectra.

References

[1] M.P.J. Verstegen, D. Radielovic, L.E. Vrenken, J. Electrochem. Soc. 121 (1974) 1627.
[2] J.L. Sommerdijk, A.N.L. Stevels, Philips Tech. Rev. 37 (1977) 221.
[3] S. Oshio, T. Matsuoka, S. Tanaka, H. Kobyashi, J. Electrochem. Soc. 145 (1998) 3903.
[4] S. Zhang, Y. Hou, T. Onishi, M. Kokubu, M. Obata, H. Tanno, T. Kono, H. Uchike, Jpn. J. Appl. Phys. 42 (2003) 477.
[5] K. Yokota, S.X. Zhang, K. Kimura, A. Sakomoto, J. Lumin. 92 (2001) 223.
[6] K.C. Mishra, M. Raukas, A. Ellens, K.H. Johnson, J. Lumin. 96 (2002) 95.
[7] P. Boolchand, K.C. Mishra, M. Raukas, A. Ellens, P.C. Schimdt, Phys. Rev. B 66 (2002) 134429.
[8] A. Ellens, F. Zwaschka, F. Kummer, A. Meijerink, M. Raukas, K. Mishra, J. Lumin. 93 (2001) 147.
[9] ICDD Powder Diffraction File, Card No.26-0163.
[10] ICDD Powder Diffraction File, Card No. 17-0306.
[11] ICDD Powder Diffraction File, Card No. 43-1009.
[12] J. Zhang, Z. Zhang, Z. Tang, Z. Zheng, Y. Lin, Powder Technol. 126 (2002) 161.
[13] G. Blasse, B.C. Grabmaier, Luminescent Materials, Springer-Verlag, 1994, p. 27.
[14] T. Kano, in: S. Shionoya, W.M. Yen (Eds.), Phosphor Handbook, CRC Press, Washington, DC, 1998, p. 181.
[15] V. Jubera, J.P. Chaminade, A. Garcia, F. Gullien, C. Fouassier, J. Lumin. 101 (2003) 1.
[16] G. Blasse, J. Solid State Chem. 4 (1972) 52.
[17] H.E. Hoefdraad, J. Solid State Chem. 15 (1975) 175.
[18] S. Polizzi, M. Battagliarin, M. Bettinelli, A. Speghini, G. Fagherazzi, J. Mater. Chem. 12 (2002) 742.
[19] W.J.L. Oomen, A.M.A. van Dongen, J. Non-Cryst. Solids 111 (1989) 205.
[20] J. Zhang, Z. Zhang, Z. Tang, Y. Tao, X. Long, Chem. Mater. 14 (2002) 3005.
[21] T. Kunimoto, A. Daud, I. Ozki, K. Okamoto, K. Ohmi, S. Tanaka, H. Kobayashi, Inst. Electronics, Information and Communication Engineers (IEICE) Trans. Electron E83C (2000) 1608.